

# INVERSE RECONSTRUCTION FROM OPTIMAL INPUT DATA

JESPER CARLSSON

ABSTRACT. This report concerns the problem to find optimal input data for an inverse reconstruction problem. In a classical parameter reconstruction problem the goal is to determine a spacially distributed (and optionally time dependent) coefficient of a partial differential equation from observed data. Here, the spacially dependent wave speed coefficient of the acoustic wave equation is sought, given observations of the solution on the boundary. The reconstruction of the coefficient is highly dependent on input data, *e.g.* if Neumann boundary values serve as input data it is in general not possible to determine the coefficient for all possible input data. It is shown that it is possible to formulate meaningful optimality criteria for the input data that enhances quality of the reconstructed coefficient. Both the problem of estimating the coefficient and the problem of finding optimal input data are ill-posed inverse problems and need to be regularized.

## CONTENTS

1. Introduction	1
2. Problem Formulation	2
2.1. Inverse Scattering	2
2.2. Optimal Input Data	3
2.3. Minimax Problem	3
3. Numerical Solution	4
3.1. Discretization	4
3.2. Optimality Condition	4
3.3. Minimization Problem	6
3.4. Maximization Problem	7
3.5. Results	7
Acknowledgment	8
References	8

## 1. INTRODUCTION

This paper describes a method to find optimal input data for inverse scattering problems. It is well known that inverse problems are ill-posed and need to be regularized [6]. Much of the research on inverse problems today is focused on how to regularize and to solve them efficiently. A more unusual question is how the choice of input data affects the solution to the inverse problem, and if it is possible to enhance the quality of the solution by simply choosing other input data. This question was asked in [3, 5] for time independent reconstruction problems in impedance tomography, and later for inverse scattering problems [4].

---

2000 *Mathematics Subject Classification.* 65M32.

*Key words and phrases.* Inverse Problems, Parameter Reconstruction.

Support by the Swedish Research Council grants 2002-6285 and 2002-4961, and the European network HYKE, funded by the EC as contract HPRN-CT-2002-00282, is acknowledged.

In [4], it was investigated how to best distinguish two different spacially dependent wave coefficients  $c(x)$  and  $c_0(x)$ , for the acoustic wave equation in the half space  $x_3 < 0$  in  $\mathbb{R}^3$ , from each other by using information of the downgoing and upgoing waves at the boundary  $x_3 = 0$ . As a measure of distinguishability the difference in energy flux between the upgoing fields for  $c$  and  $c_0$  was chosen, and it was shown that this difference is maximized by a time-harmonic downgoing wave with frequency depending on the two coefficients. In this paper, a similar approach is used, but with the focus on how the choice of the incoming wave affects the reconstruction for the inverse problem to reconstruct an unknown wave coefficient.

## 2. PROBLEM FORMULATION

Consider the acoustic wave equation in an bounded open domain  $\Omega \in \mathbb{R}^2$  and for times  $t \in [0, T]$ :

$$(1) \quad \begin{aligned} \varphi_{tt}^* &= \operatorname{div}(\sigma^* \nabla \varphi^*), & \text{in } \Omega \times (0, T], \\ \sigma^* \nabla \varphi^* \cdot \mathbf{n} &= j, & \text{on } \Gamma_N \times (0, T], \\ \sigma^* \nabla \varphi^* \cdot \mathbf{n} &= 0, & \text{on } \partial\Omega \setminus \Gamma_N \times (0, T], \\ \varphi^* &= \varphi_t^* = 0, & \text{on } \bar{\Omega} \times \{t = 0\}, \end{aligned}$$

where  $\varphi^* : \bar{\Omega} \times [0, T] \rightarrow \mathbb{R}$  denotes acoustic pressure,  $\sigma^* : \bar{\Omega} \rightarrow \mathbb{R}$ ,  $\sigma^* > 0$  is the squared wave speed and  $\Gamma_N \subseteq \partial\Omega$ . To find the acoustic pressure  $\varphi^*$ , for a given coefficient  $\sigma^*$  and boundary data  $j : \Gamma_N \times (0, T] \rightarrow \mathbb{R}$ , is the *forward* problem. Given sufficient regularity of the input data, *e.g.*  $\sigma^* \in C^1(\Omega)$  and  $j \in L^2(0, T; L^2(\Gamma_N))$ , the forward problem is well posed, *i.e.* there exists a unique (weak) solution  $\varphi \in L^2(0, T; H^1(\Omega))$  which depends continuously on  $j$  and  $\sigma^*$ , see [7]. A typical corresponding *inverse* problem to (1) is to find  $\sigma^*$ , for given input boundary data  $j$  and measurements  $\varphi^*$ .

**2.1. Inverse Scattering.** Unlike the forward problem above, the inverse problem is ill posed, *i.e.* there may not exist a solution  $\sigma^*$ , and if it exists it may not be unique nor depend continuously on the data  $j$  and  $\varphi^*$ . To formulate an inverse problem that has a unique solution, with continuous dependence on data, it is necessary to add some regularization [6].

The *regularized* inverse scattering problem is here: for given Neumann boundary data  $j$  and measurements  $\varphi^*$  on  $\Gamma_M \subset \partial\Omega$ , find the coefficient  $\sigma : \bar{\Omega} \rightarrow \mathbb{R}$ ,  $\sigma > 0$ , and the state  $\varphi : \bar{\Omega} \times [0, T] \rightarrow \mathbb{R}$ , that minimizes the error functional

$$(2) \quad \frac{1}{2} \int_0^T \int_{\Gamma_M} (\varphi - \varphi^*)^2 \, ds \, dt + \frac{\delta}{2} \int_{\Omega} (\sigma^2 + |\nabla \sigma|^2) \, dx,$$

and satisfies the acoustic wave equation

$$(3) \quad \begin{aligned} \varphi_{tt} &= \operatorname{div}(\sigma \nabla \varphi), & \text{in } \Omega \times (0, T], \\ \sigma \nabla \varphi \cdot \mathbf{n} &= j, & \text{on } \Gamma_N \times (0, T], \\ \sigma \nabla \varphi \cdot \mathbf{n} &= 0, & \text{on } \partial\Omega \setminus \Gamma_N \times (0, T], \\ \varphi &= \varphi_t = 0, & \text{on } \bar{\Omega} \times \{t = 0\}. \end{aligned}$$

The second term in (2) is a Tikhonov regularization, with  $\delta > 0$ , that ensures that the minimization problem is well posed [7]. Also, it is assumed that the measurements  $\varphi^*$  satisfy (1) for some unknown  $\sigma^*$ .

Note that, for simplicity a pure Neumann boundary condition is here used, but it is possible to use a Dirichlet condition on a subset  $\Gamma_D \subset \partial\Omega$ ,  $\Gamma_D \cap \Gamma_M \neq \Gamma_M$ , without complication.

**2.2. Optimal Input Data.** The objective of this paper is not only to solve the above minimization problem (2), but also to find the best possible boundary input data  $j$  that ensures a good reconstruction of  $\sigma^*$ . For the acoustic wave equation the choice of input data is highly important since a wave may only visit a subset of the region  $\Omega$  before it is measured, and it can thus only be expected to find an approximation of  $\sigma^*$  in that subset.

One way to define what is meant by the "best" input  $j$  is to first define the concept of distinguishability, *i.e.* how to best distinguish two coefficients  $\sigma$  and  $\sigma^*$  from each other. Following [3], let  $\Lambda_\sigma$  denote the Neumann-to-Dirichlet map

$$\Lambda_\sigma : \sigma \frac{\partial \varphi}{\partial n} \Big|_{\partial\Omega \times (0,T]} \rightarrow \varphi|_{\partial\Omega \times (0,T]}$$

which associates the input  $j$  with the solution  $\varphi$  on the boundary, and define the distinguishability as

$$d(\sigma, \sigma^*) := \frac{\|(\Lambda_\sigma - \Lambda_{\sigma^*})j\|_{\partial\Omega \times (0,T)}}{\|j\|_{\partial\Omega \times (0,T)}} = \frac{\|\varphi - \varphi^*\|_{\partial\Omega \times (0,T)}}{\|j\|_{\partial\Omega \times (0,T)}},$$

where  $\|\cdot\|_A$  denotes the  $L^2(A)$  norm with corresponding inner product  $(\cdot, \cdot)_A$ . Here, the  $L^2$  norm was chosen for simplicity, but it may happen that two coefficients that are not distinguishable in the  $L^2$  norm are still distinguishable in norms that better reflect the regularity of  $j$  and  $\varphi$ , see [3].

Given  $\sigma$  and  $\sigma^*$ , the best input  $j$  can be defined as the maximizer to  $d(\sigma, \sigma^*)$ , *i.e.* the eigenfunction that corresponds to the dominating eigenvalue of the difference operator  $\Lambda_\sigma - \Lambda_{\sigma^*}$ . To find the eigenfunction for the dominating eigenvalue, power iteration can be used, an approach that was used in [2] to find good input currents for impedance tomography.

**2.3. Minimax Problem.** If the Neumann data  $j$  is normalized by introducing a new variable  $q : \Gamma_N \times (0, T] \rightarrow \mathbb{R}$  such that

$$j := \frac{q}{\|q\|_{\Gamma_N \times (0,T]}}, \quad \text{on } \Gamma_N \times (0, T],$$

the problem to find both the coefficient  $\sigma^*$  and an optimal input  $j$  can be formulated as the minimax problem

$$(4) \quad \min_{\sigma} \max_q \|\varphi - \varphi^*\|_{\Gamma_M \times (0,T]}^2 + \frac{\delta}{2} \left( \|\sigma\|_{\Omega}^2 + \|\nabla \sigma\|_{\Omega}^2 \right),$$

with the constraints (1) and (3). Remember, that since  $\sigma^*$  is unknown Equation (3) cannot be solved, but the measurements  $\varphi^*$  on the boundary are still accessible through experiments.

Similarly to the minimization of (4), the maximization is an inverse problem and can be expected to be ill posed. The normalization of  $j$  here acts as a Tikhonov regularization, and ensures that the objective function is bounded, but it is not clear if the maximization admits a solution, or if the solution is unique. Additional regularization may thus be needed. In Section 3.5, it is observed that  $q$  and correspondingly  $\varphi$  tends to oscillate in time as the measurement error grows, and to prevent large oscillations the numerical method is interrupted prematurely. An alternative measure would be to add a penalty on the time derivative of  $q$  in (4). Physically, it would also be suitable to include a constraint on the energy, as in [4], but this approach is not pursued in this paper.

Since the concavity with respect to  $q$  is unclear, the minimization and maximization problems will here be treated as two separate subproblems:

**Max:** Given  $\sigma$  and  $\sigma^*$ , maximize (4) with respect to  $j$  under the constraints (1) and (3).

**Min:** Given  $j$  and  $\varphi^*$ , minimize (4) with respect to  $\sigma$  under the constraint (3).

Even if the min and max in (4) could switch place, there are numerical considerations which leads to two separate subproblems. This will be explained in the following sections.

### 3. NUMERICAL SOLUTION

**3.1. Discretization.** Let  $V \subset H^1(\Omega)$  be the finite element subspace of continuous piecewise linear functions on a triangular finite element mesh on  $\Omega$ , and divide the interval  $[0, T]$  into  $N$  intervals of equal length  $k = T/N$ . An explicit scheme, discretized in time and finite elements in space, for the weak form of Equation (3) is

$$(5) \quad \begin{aligned} (\varphi_{n+1} - 2\varphi_n + \varphi_{n-1}, v)_\Omega &= k^2(j_n, v)_{\Gamma_N} - k^2(\sigma \nabla \varphi_n, \nabla v)_\Omega, \quad \forall v \in V, \\ \varphi_0 &= \varphi_1 = 0, \end{aligned}$$

for  $n = 1, \dots, N-1$ . Also, even though Equation (1) is never solved computationally, since  $\varphi^*$  is measured, it is assumed that the measured data uses the same discretization

$$(6) \quad \begin{aligned} (\varphi_{n+1}^* - 2\varphi_n^* + \varphi_{n-1}^*, v)_\Omega &= k^2(j_n, v)_{\Gamma_N} - k^2(\sigma^* \nabla \varphi_n^*, \nabla v)_\Omega, \quad \forall v \in V, \\ \varphi_0^* &= \varphi_1^* = 0, \end{aligned}$$

for  $n = 1, \dots, N-1$ . Using formulation (4) above, with Neumann boundary data  $j_n$  defined by

$$j_n := \frac{q_n}{\sqrt{k \sum_{n=1}^{N-1} \|q_n\|_{\Gamma_N}^2}},$$

the discretized minimax problem is thus to find  $\varphi_2, \dots, \varphi_N, \varphi_2^*, \dots, \varphi_N^*, q_1, \dots, q_{N-1}$  and  $\sigma$  such that

$$(7) \quad \min_{\sigma} \max_{q_1, \dots, q_{N-1}} \frac{k}{2} \sum_{n=0}^N \|\varphi_n - \varphi_n^*\|_{\Gamma_M}^2 + \frac{\delta}{2} (\|\sigma\|_\Omega^2 + \|\nabla \sigma\|_\Omega^2),$$

under the constraints (5) and (6).

**3.2. Optimality Condition.** To formulate an optimality condition for the discretized problem (7), (5) and (6), the Lagrangian is introduced:

$$\begin{aligned} L := & \frac{k}{2} \sum_{n=0}^N \|\varphi_n - \varphi_n^*\|_{\Gamma_M}^2 + \frac{\delta}{2} (\|\sigma\|_\Omega^2 + \|\nabla \sigma\|_\Omega^2) + \\ & + \sum_{n=1}^{N-1} \frac{1}{k} (\varphi_{n+1} - 2\varphi_n + \varphi_{n-1}, \lambda_{n-1})_\Omega - k(j_n, \lambda_{n-1})_{\Gamma_N} + k(\sigma \nabla \varphi_n, \nabla \lambda_{n-1})_\Omega \\ & + \sum_{n=1}^{N-1} \frac{1}{k} (\varphi_{n+1}^* - 2\varphi_n^* + \varphi_{n-1}^*, \lambda_{n-1}^*)_\Omega - k(j_n, \lambda_{n-1}^*)_{\Gamma_N} + k(\sigma^* \nabla \varphi_n^*, \nabla \lambda_{n-1}^*)_\Omega \end{aligned}$$

with multipliers  $\lambda_n, \lambda_n^* \in V, n = 0, \dots, N-2$ .

An optimal solution to the discretized minimax problem is also stationary point to the Lagrangian, and satisfies

$$(8) \quad \begin{aligned} \partial_{\varphi_{n+1}} L &= 0, & \partial_{\lambda_{n-1}} L &= 0, \\ \partial_{\varphi_{n+1}^*} L &= 0, & \partial_{\lambda_{n-1}^*} L &= 0, \\ \partial_{q_n} L &= 0, & \partial_{\sigma} L &= 0, \end{aligned}$$

for  $n = 1, \dots, N-1$ . The variation with respect to  $\lambda_{n-1}$  and  $\lambda_{n-1}^*$  in (8) becomes Equation (5) and (6), respectively. Variation in  $\varphi_{n+1}$  and  $\varphi_{n+1}^*$  gives the adjoint equations

$$(9) \quad \begin{aligned} (\lambda_{n+1} - 2\lambda_n + \lambda_{n-1}, v)_\Omega &= -k^2(\varphi_{n+1} - \varphi_{n+1}^*, v)_{\Gamma_M} - k^2(\sigma \nabla \lambda_n, \nabla v)_\Omega, \\ \lambda_N &= \lambda_{N-1} = 0, \end{aligned}$$

and

$$(10) \quad \begin{aligned} (\lambda_{n+1}^* - 2\lambda_n^* + \lambda_{n-1}^*, v)_\Omega &= k^2(\varphi_{n+1} - \varphi_{n+1}^*, v)_{\Gamma_M} - k^2(\sigma^* \nabla \lambda_n^*, \nabla v)_\Omega, \\ \lambda_N^* &= \lambda_{N-1}^* = 0, \end{aligned}$$

for all  $v \in V$ . Stationarity with respect to  $q_n$  and  $\sigma$  is given by

$$(11) \quad \frac{k^2(q_n, \lambda_{n-1} + \lambda_{n-1}^*)_{\Gamma_N} (q_n, v)_{\Gamma_N}}{\left(k \sum_{n=1}^{N-1} \|q_n\|_{\partial\Omega}^2\right)^{\frac{3}{2}}} - \frac{k(\lambda_{n-1} + \lambda_{n-1}^*)_{\Gamma_N}}{\left(k \sum_{n=1}^{N-1} \|q_n\|_{\Gamma_N}^2\right)^{\frac{1}{2}}} = 0,$$

and

$$(12) \quad \delta(\sigma, v)_\Omega + \delta(\nabla \sigma, \nabla v)_\Omega + k \sum_{n=1}^{N-1} (v \nabla \varphi_n, \nabla \lambda_{n-1})_\Omega = 0,$$

respectively, for all  $v \in V$ . For simplicity, it is here assumed that  $\sigma, q_n \in V$ .

Expressions (9) and (10) are discretizations of the adjoint equations

$$(13) \quad \begin{aligned} \lambda_{tt} &= \operatorname{div}(\sigma \nabla \lambda), & \text{in } \Omega \times [0, T], \\ \sigma \nabla \lambda \cdot \mathbf{n} &= -(\varphi - \varphi^*), & \text{on } \Gamma_M \times [0, T], \\ \sigma \nabla \lambda \cdot \mathbf{n} &= 0, & \text{on } \partial\Omega \setminus \Gamma_M \times [0, T], \\ \lambda &= \lambda_t = 0, & \text{on } \bar{\Omega} \times \{t = T\}, \end{aligned}$$

and

$$(14) \quad \begin{aligned} \lambda_{tt}^* &= \operatorname{div}(\sigma^* \nabla \lambda^*), & \text{in } \Omega \times [0, T], \\ \sigma^* \nabla \lambda^* \cdot \mathbf{n} &= (\varphi - \varphi^*), & \text{on } \Gamma_M \times [0, T], \\ \sigma^* \nabla \lambda^* \cdot \mathbf{n} &= 0, & \text{on } \partial\Omega \setminus \Gamma_M \times [0, T], \\ \lambda^* &= \lambda_t^* = 0, & \text{on } \bar{\Omega} \times \{t = T\}, \end{aligned}$$

but compared to the discretization of the forward problem (3) the boundary conditions are evaluated at a different time step. Equation (12) is an approximation to the equation

$$(15) \quad \begin{aligned} \delta(\Delta \sigma - \sigma) &= \int_0^T \nabla \varphi \cdot \nabla \lambda \, dt, & \text{in } \Omega, \\ \nabla \sigma \cdot \mathbf{n} &= 0, & \text{on } \partial\Omega. \end{aligned}$$

Observe, that since  $\sigma^*$  is unknown neither (1), (14) nor their discretized counterparts (6), (10) can be solved. However, it is possible to experimentally apply the appropriate Neumann boundary conditions and measure the resulting boundary values  $\varphi^*$  and  $\lambda^*$ .

The fact that  $\varphi^*$ ,  $\lambda^*$  and  $\sigma^*$  are not accessible in  $\Omega$  makes it hard to solve the optimality system (8) efficiently since not all of the second variations of the Lagrangian are accessible. Also, as mentioned in Section 2.3, the minimax problem may not be convex-concave, so to simultaneously solve the equations in (8) may not give the same results as treating the minimization and maximization separately. The regularized minimization problem is convex in a neighbourhood of the optimal  $\sigma$  and all second variations are accessible, so Newton's method can be used. However, for the maximization problem none of the second variations are available.

**3.3. Minimization Problem.** Assume that Neumann boundary data  $j$  and measurements  $\varphi^*$  are given. The forward equation (5) for  $\varphi$ , the dual equation (9) for  $\lambda$  and the steady state equation (12) for  $\sigma$  can be written as

$$\begin{aligned} f_n &:= \frac{1}{k}(\lambda_{n+1} - 2\lambda_n + \lambda_{n-1}, v)_\Omega + k(\varphi_{n+1} - \varphi_{n+1}^*, v)_{\Gamma_M} + k(\sigma \nabla \lambda_n, \nabla v)_\Omega &= 0 \\ g_n &:= \frac{1}{k}(\varphi_{n+1} - 2\varphi_n + \varphi_{n-1}, v)_\Omega - k(j_n, v)_{\Gamma_N} + k(\sigma \nabla \varphi_n, \nabla v)_\Omega &= 0 \\ h &:= \delta(\sigma, v)_\Omega + \delta(\nabla \sigma, \nabla v)_\Omega + k \sum_{i=1}^{N-1} (v \nabla \varphi_i, \nabla \lambda_{i-1})_\Omega &= 0 \end{aligned}$$

for  $n = 1, \dots, N-1$  and  $\forall v \in V$ . The Newton method for finding the stationary point to the above system is to, given  $\varphi$ ,  $\lambda$  and  $\sigma$ , find the updates  $\hat{\varphi} := (\hat{\varphi}_2, \dots, \hat{\varphi}_N)^T$ ,  $\hat{\lambda} := (\hat{\lambda}_0, \dots, \hat{\lambda}_{N-2})^T$  and  $\hat{\sigma}$  that satisfies

$$\begin{aligned} k(\hat{\varphi}_{n+1}, v)_{\Gamma_M} + \frac{1}{k}(\hat{\lambda}_{n+1} - 2\hat{\lambda}_n + \hat{\lambda}_{n-1}, v)_\Omega + \\ + k(\sigma \nabla \hat{\lambda}_n + \hat{\sigma} \nabla \lambda_n, \nabla v)_\Omega &= -f_n, \quad n = 1, \dots, N-3, \\ k(\hat{\varphi}_{n+1}, v)_{\Gamma_M} + \frac{1}{k}(-2\hat{\lambda}_n + \hat{\lambda}_{n-1}, v)_\Omega + \\ + k(\sigma \nabla \hat{\lambda}_n + \hat{\sigma} \nabla \lambda_n, \nabla v)_\Omega &= -f_n, \quad n = N-2, \\ k(\hat{\varphi}_{n+1}, v)_{\Gamma_M} + \frac{1}{k}(\hat{\lambda}_{n-1}, v)_\Omega + k(\hat{\sigma} \nabla \lambda_n, \nabla v)_\Omega &= -f_n, \quad n = N-1, \\ \frac{1}{k}(\hat{\varphi}_{n+1}, v)_\Omega + k(\hat{\sigma} \nabla \varphi_n, \nabla v)_\Omega &= -g_n, \quad n = 1, \\ \frac{1}{k}(\hat{\varphi}_{n+1} - 2\hat{\varphi}_n, v)_\Omega + k(\sigma \nabla \hat{\varphi}_n + \hat{\sigma} \nabla \varphi_n, \nabla v)_\Omega &= -g_n, \quad n = 2, \\ \frac{1}{k}(\hat{\varphi}_{n+1} - 2\hat{\varphi}_n + \hat{\varphi}_{n-1}, v)_\Omega + k(\sigma \nabla \hat{\varphi}_n + \hat{\sigma} \nabla \varphi_n, \nabla v)_\Omega &= -g_n, \quad n = 3, \dots, N-1, \end{aligned}$$

and

$$k \sum_{n=2}^{N-1} (v \nabla \hat{\varphi}_n, \nabla \lambda_{n-1})_\Omega + k \sum_{n=1}^{N-1} (v \nabla \varphi_n, \nabla \hat{\lambda}_{n-1})_\Omega + \delta(\hat{\sigma}, v)_\Omega + \delta(\nabla \hat{\sigma}, \nabla v)_\Omega = -h,$$

for all  $v \in V$ , or in matrix notation

$$(16) \quad \begin{pmatrix} K_{11} & K_{12} & K_{13} \\ K_{12}^T & 0 & K_{23} \\ K_{13}^T & K_{23}^T & K_{33} \end{pmatrix} \begin{pmatrix} \hat{\varphi} \\ \hat{\lambda} \\ \hat{\sigma} \end{pmatrix} = - \begin{pmatrix} f \\ g \\ h \end{pmatrix}.$$

where  $f := (f_1, \dots, f_{N-1})^T$  and  $g := (g_1, \dots, g_{N-1})^T$ .

Let  $M$ ,  $\bar{M}$ ,  $S(\sigma)$  and  $P(\varphi)$  be matrices with the elements

$$\begin{aligned} M_{ij} &= (v_i, v_j)_\Omega, & \bar{M}_{ij} &= (v_i, v_j)_{\partial\Omega}, \\ S_{ij}(\sigma) &= (\sigma \nabla v_i, \nabla v_j)_\Omega, & P_{ij}(\varphi) &= (v_j \nabla \varphi, \nabla v_i)_\Omega, \end{aligned}$$

where  $v_i$  denotes the basis functions of the finite element space  $V$ , then the submatrices in the Newton system (16) are of the form (for  $N = 4$ )

$$K_{11} = k \begin{pmatrix} \bar{M} & & \\ & \bar{M} & \\ & & \bar{M} \end{pmatrix}, \quad K_{12} = \frac{1}{k} \begin{pmatrix} M & k^2 S(\sigma) - 2M & M \\ & M & k^2 S(\sigma) - 2M \\ & & M \end{pmatrix},$$

and

$$K_{13} = k \begin{pmatrix} P(\lambda_1) \\ P(\lambda_2) \\ P(\lambda_3) \end{pmatrix}, \quad K_{23} = k \begin{pmatrix} P(\varphi_1) \\ P(\varphi_2) \\ P(\varphi_3) \end{pmatrix}, \quad K_{33} = \delta(M + S(1)).$$

To solve the Newton system (16) with a direct solver is very demanding for large problems and in practice it must be done iteratively. For the examples in this report, the GMRES method with a simple preconditioner, was used. The preconditioner is based on solving the system approximately, for an arbitrary right hand side  $(f, g, h)$ , with the Gauss-Seidel method, *i.e.* given  $(\hat{\varphi}^i, \hat{\lambda}^i, \hat{\sigma}^i)$  an approximate solution is given by iterating according to the scheme

$$\begin{aligned} K_{12}^T \hat{\varphi}^{i+1} &= g - K_{23} \hat{\sigma}^i, \\ K_{11} \hat{\varphi}^{i+1} + K_{12} \hat{\lambda}^{i+1} &= f - K_{13} \hat{\sigma}^i, \\ K_{13}^T \hat{\varphi}^{i+1} + K_{23}^T \hat{\lambda}^{i+1} + K_{33} \hat{\sigma}^{i+1} &= h. \end{aligned}$$

For the examples in Section 3.5, it turned out that one single iteration with the Gauss-Seidel method provided a sufficiently good preconditioner to achieve acceptable convergence with the GMRES method. This could not be done with any of the standard algebraic preconditioners like Jacobi, ILU or SOR, which worked poorly due to the block structure of the Newton system.

To achieve reasonable convergence for larger problems a more clever approach is needed. One idea is to use the approximate Gauss-Newton system

$$(17) \quad \begin{pmatrix} K_{11} & K_{12} & 0 \\ K_{12}^T & 0 & K_{23} \\ 0 & K_{23}^T & K_{33} \end{pmatrix} \begin{pmatrix} \hat{\varphi} \\ \hat{\lambda} \\ \hat{\sigma} \end{pmatrix} = - \begin{pmatrix} f \\ g \\ h \end{pmatrix}.$$

which arises from the observation that  $\lambda \approx 0$  close to an optimum. A preconditioner can be derived from (17) by noting that eliminating  $\hat{\varphi}$  and  $\hat{\lambda}$  from (17) leads to the reduced system

$$(18) \quad \underbrace{(K_{33} + K_{23}^T K_{12}^{-1} K_{11} K_{12}^{-T} K_{23})}_{H_r} \hat{\sigma} = K_{23}^T K_{12}^{-1} (f - K_{11} K_{12}^{-T} g) - h.$$

with a symmetric positive definite reduced Hessian  $H_r$  which then can be approximated by *e.g.* a quasi-Newton method, see [1].

**3.4. Maximization Problem.** Given  $\sigma$ , the maximization problem is solved by the gradient method:

- a. Start with an initial guess  $q^i$ .
- b. Solve the forward equation (5) and the dual equation (9) to get  $\varphi$  and  $\lambda$ .
- c. Apply the Neumann boundary values  $j$  (given by  $q^i$ ) and  $-\varphi + \varphi^*$  to the physical system (1) with unknown coefficient  $\sigma^*$ , and *measure* the resulting boundary values  $\varphi^*$  and  $\lambda^*$ , respectively.
- d. Take a step in the gradient direction in  $q$  *i.e.*

$$q_n^{i+1} = q_n^i + \alpha \partial_{q_n} L,$$

for  $n = 1, \dots, N-1$ ,  $\alpha \in (0, 1]$ , and with  $\partial_{q_n} L$  given by the left hand side of (11).

- e. Goto step (a) unless tolerance is achieved or oscillations in  $q$  become too large.

**3.5. Results.** In the following examples a slightly different objective function

$$(19) \quad \max_q \frac{\|\varphi - \varphi^*\|_{\Gamma_M \times (0, T)}^2}{\|\varphi\|_{\Gamma_M \times (0, T)}^2}.$$

is used for the maximization problem but not for the minimization problem. Even though  $\varphi$  is bounded in the  $L^2$  norm on  $\Gamma_M \times (0, T)$  it may be a good idea restrict  $\varphi$  even more. This does however not change the generality of the previous sections other than changing the boundary values  $\sigma \nabla \lambda \cdot \mathbf{n}$  and  $\sigma^* \nabla \lambda^* \cdot \mathbf{n}$  on  $\Gamma_M \times [0, T)$

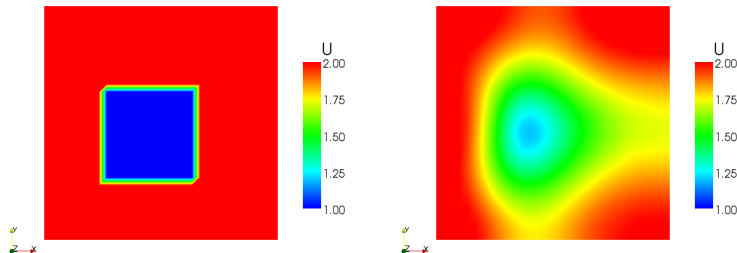


FIGURE 1. Left: The sought coefficient  $\sigma^*$ . Right:  $\sigma$  after first minimization. Boundary data:  $q = \sin(2\pi t) \sin(\pi y)$  at  $x = 0$ .

when performing the maximization. Also, the results do not differ much from using the original objective function (4).

In Figure 1 to 6, three different examples are shown. In all examples a wave coefficient  $\sigma^*$  is reconstructed in the unit square by sending in a wave at  $\Gamma_N \times (0, T] := \{x = 0\} \times (0, 1]$  and measuring the acoustic pressure  $\varphi^*$  at  $\Gamma_M \times (0, T] := \{x = 0\} \times (0, 1] \cup \{x = 1\} \times (0, 1]$ . First, the minimization problem is solved for a small regularization  $\delta = 10^{-5}$ , then the calculated  $\sigma$  is used to maximize (19) with respect to  $q$ . Before the maximization the incoming wave is modelled by  $q = \sin(2\pi t) \sin(\pi y)$ , in Figures 1 and 3, and  $q = \sin(\pi t) \sin(\pi y)$  in Figure 5. Finally, the minimization problem is solved again but with Neumann data  $j$  given by the new  $q$ . Of course, this can be done repeatedly and it is not necessary to start by solving the minimization problem, but instead start with some qualified guess for  $\sigma$ .

The Newton method for the minimization problem is solved such that the absolute residual error is less than  $10^{-13}$  and the gradient method for the maximization problem is terminated when the  $L^2$  norm of  $j_t$  gets to big. The calculations were done on a uniform triangular mesh with 1800 triangles and 125 time steps, and the measurements were simulated by using the same mesh.

The left part of Figure 1, 3 and 5 show the unknown coefficient  $\sigma^*$ , and the right part of the figures show  $\sigma$  after the first minimization. Figure 2, 4 and 6 show  $\sigma$  after the second minimization. In Figure 7 the simulated solution  $\varphi^*$  is shown before and after the maximization in  $q$ .

#### ACKNOWLEDGMENT

I am grateful to Anders Szepessy for his insightful ideas and helpful comments on this work.

#### REFERENCES

- [1] George Biros and Omar Ghattas. Parallel Lagrange-Newton-Krylov-Schur methods for PDE-constrained optimization. I. The Krylov-Schur solver. *SIAM J. Sci. Comput.*, 27(2):687–713 (electronic), 2005.
- [2] Jesper Carlsson, Mattias Sandberg, and Anders Szepessy. Symplectic pontryagin approximations for optimal design. Preprint.
- [3] Margaret Cheney and David Isaacson. Distinguishability in impedance imaging. *IEEE Trans. Biomed. Eng.*, 39(8):852–860, 1992.
- [4] Margaret Cheney, David Isaacson, and Matti Lassas. Optimal acoustic measurements. *SIAM J. Appl. Math.*, 61(5):1628–1647 (electronic), 2001.
- [5] Margaret Cheney, David Isaacson, and Jonathan C. Newell. Electrical impedance tomography. *SIAM Rev.*, 41(1):85–101 (electronic), 1999.



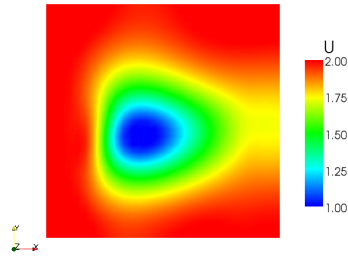


FIGURE 2. The coefficient  $\sigma$  after the second minimization. In the maximization of  $q$ , the value function increased 600% and the  $L^2$  norm of  $q_t$  increased 100%. The decrease in the  $L^2(\Omega)$  norm of  $\sigma - \sigma^*$  between the first and second minimization was 30%.

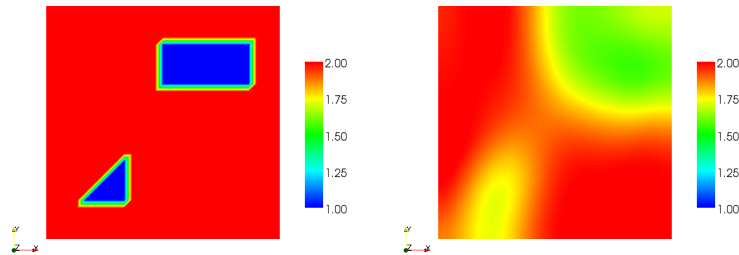


FIGURE 3. Left: The sought coefficient  $\sigma^*$ . Right:  $\sigma$  after first minimization. Boundary data:  $q = \sin(2\pi t) \sin(\pi y)$  at  $x = 0$ .

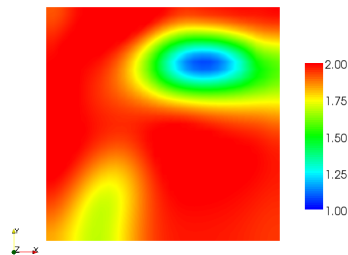


FIGURE 4. The coefficient  $\sigma$  after the second minimization. In the maximization of  $q$ , the value function increased 1200% and the  $L^2$  norm of  $q_t$  increased 100%. The decrease in the  $L^2(\Omega)$  norm of  $\sigma - \sigma^*$  between the first and second minimization was 32%.

- [6] Heinz W. Engl, Martin Hanke, and Andreas Neubauer. *Regularization of inverse problems*, volume 375 of *Mathematics and its Applications*. Kluwer Academic Publishers Group, Dordrecht, 1996.
- [7] J.-L. Lions. *Optimal control of systems governed by partial differential equations*. Translated from the French by S. K. Mitter. Die Grundlehren der mathematischen Wissenschaften, Band 170. Springer-Verlag, New York, 1971.

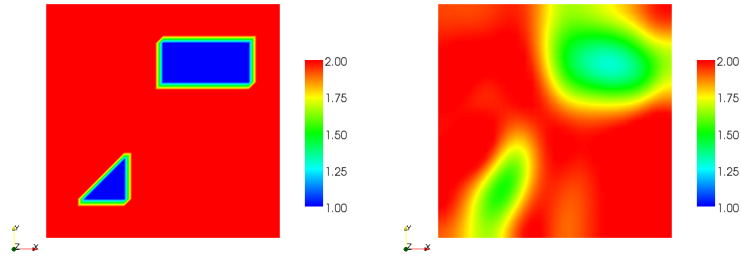


FIGURE 5. Left: The sought coefficient  $\sigma^*$ . Right:  $\sigma$  after first minimization. Boundary data:  $q = \sin(\pi t) \sin(\pi y)$  at  $x = 0$ .

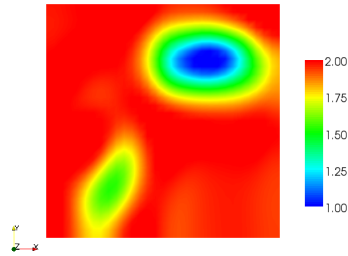


FIGURE 6. The coefficient  $\sigma$  after the second minimization. In the maximization of  $q$ , the value function increased 400% and the  $L^2$  norm of  $q_t$  increased 50%. The decrease in the  $L^2(\Omega)$  norm of  $\sigma - \sigma^*$  between the first and second minimization was 40%.

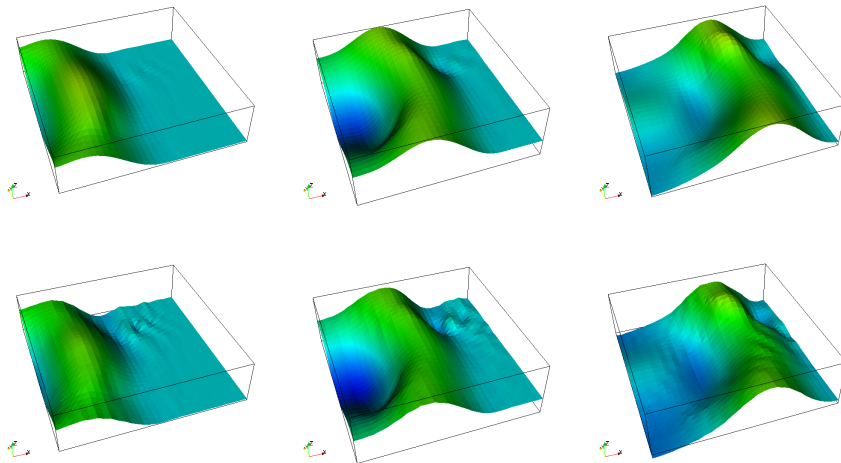


FIGURE 7. The measured solution  $\varphi^*$  before (top) and after (bottom) the maximization in  $q$ , for three different timesteps. The oscillations in  $q$  after the maximization are clearly visible in  $\varphi^*$ .

CSC, NUMERICAL ANALYSIS, KUNGL. TEKNISKA HÖGSKOLAN, 100 44 STOCKHOLM, SWEDEN;  
*E-mail address:* **jesperc@kth.se**